NEARSHORE, WAVE AND TOPOGRAPHIC EFFECTS IN STORM SURGES

Gary Watson[1] and Takao Yamashita [2]

Abstract

Some ideas for improving the accuracy of storm surge prediction models are discussed. A detailed coastal flooding model is applied to the flooding of Chittagong in the April 1991 disaster, but results are only illustrative due to the lack of good topography data. The influence of waves on wind stress forcing and bottom friction is discussed. Some recent results from a coastal observation tower taken during a typhoon show enhanced stress compared with values from empirical formulae in the literature. A new model for improving the representation of typhoon wind fields in areas surrounded by mountains is presented. Its applicability for storm surge computation is demonstrated using observations of a typhoon and surge in Osaka Bay.

Introduction

Storm surges, abnormal rises in sea level cause by strong onshore winds, pose one of the most severe natural hazards in many coastal areas. As recently as 1991, 150,000 people died in Bangladesh, mostly by drowning in coastal floods caused by a severe cyclone and surge. Effective action to minimize the impact of such disasters depends on advance knowledge of the threat to any particular location. A number of numerical models have been developed for predicting surges, and in some countries they are used operationally for making surge warnings. However, there remains scope for improving the representation of a number of phenomena in the models and this paper describes some recent investigations. These include new work on modelling coastal flooding; modelling of the wave field and its effects

---

[1]Cooperative Foreign Researcher, Disaster Prevention Research Institute, Kyoto University, Gokasho, Uji, Kyoto 611, Japan
[2]Associate Professor, same address.

on wind stress, bottom friction and coastal set-up; and the effect of mountains on the wind field.

Surge models commonly use some form of the non-linear shallow-water equations for mass and momentum conservation, with appropriate forcing terms. Here we use the following:

$$\frac{\partial \zeta}{\partial t} + \frac{\partial (ud)}{\partial x} + \frac{\partial (vd)}{\partial y} = 0 \tag{1}$$

$$\frac{\partial u}{\partial t} + u\frac{\partial u}{\partial x} + v\frac{\partial u}{\partial y} = fv - g\frac{\partial \zeta}{\partial x} - \frac{1}{\rho}\frac{\partial p_a}{\partial x} + \frac{1}{\rho d}\tau_{sx} - \frac{1}{\rho d}\tau_{bx} + A\nabla^2 u \tag{2}$$

$$\frac{\partial v}{\partial t} + u\frac{\partial v}{\partial x} + v\frac{\partial v}{\partial y} = -fu - g\frac{\partial \zeta}{\partial y} - \frac{1}{\rho}\frac{\partial p_a}{\partial y} + \frac{1}{\rho d}\tau_{sy} - \frac{1}{\rho d}\tau_{by} + A\nabla^2 v \tag{3}$$

where ζ is surface elevation, d is total water depth, and (u, v) is depth-averaged velocity. The terms on the right of the momentum equations (2) and (3) are due respectively to Coriolis force, surface slope, atmospheric pressure gradient, surface wind stress $\vec{\tau}_s = (\tau_{sx}, \tau_{sy})$, bottom friction stress $\vec{\tau}_b = (\tau_{bx}, \tau_{by})$, and eddy viscosity. A is an eddy viscosity coefficient.

If the wind field is reasonably well approximated, the storm surge predicted by models based on these equations is generally good enough to be useful. In principle however, it is possible to make improvements to the methods currently used. In the case of surges generated by tropical storms, the main limitation is the accuracy of storm forecasts. Prediction of the storm's track and speed are especially important, because landfall point and timing relative to local high tide strongly affect the location and depth of flooding (Flather, 1994). Storm intensity is also a primary factor determining surge height and this too is difficult to forecast, as it can change unexpectedly. Any progress in these respects would improve the surge forecasts.

Besides this, there are other improvements which could be made. Figure 1 illustrates some phenomena that occur during storm surges, which are not normally included in the models. Those discussed briefly in this paper are the flooding of rivers and low-lying coastal land, including the possibility of bore formation; the effect of waves on the wind stress, bottom stress and coastal set-up; and the effect of mountains on the wind field. Others that are not discussed here include coastal wave hazard, the drag effects of terrain, vegetation and buildings on flooding, changes in river levels (especially when in flood), and morphodynamic changes due to sediment transport during the surge. Ideally, all of these effects should be incorporated into future operational surge models.

Flooding of Rivers and Low-Lying Coastal Land

The most dangerous threat during a storm surge is the sudden flooding of inahabited areas on land near the coast. It is thus highly desirable to be able to model and predict such events in as much detail as possible. A standard surge model with a fixed boundary is able to make a reasonable prediction of the
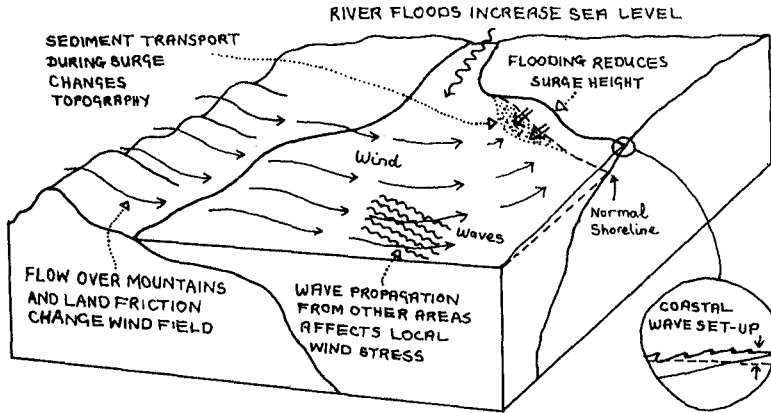
Figure 1: Some phenomena that occur during storm surges.

increase in coastal sea level, but this does not tell us the extent of flooding to be expected in any particular area. For example, if there is a river or an extensive area of low-lying land, the flooding will reach further inland and pose a more severe hazard. For flooding studies, we can use a local model with a fine grid covering the area of interest. Here we present some preliminary results from a model which is under development, simulating the flooding of Chittagong during the April 1991 disaster in Bangladesh.

A number of reports have said that surges in the Bay of Bengal are sometimes observed as "walls of water", suggesting that they may steepen and break in the same way as a tidal bore. Tides and tsunamis are well known for steepening into breaking bores in suitably-shaped estuaries and rivers. It is likely that this may also sometimes happen with storm surges. The sudden increase in water level and associated turbulence would increase the resulting danger, and it is thus important to understand and be able to predict the circumstances under which bore formation can occur.

We thus use a model for coastal flooding that is able to represent bore formation. It is based on the nonlinear shallow-water equations and uses a numerical method which accurately handles the formation of discontinuities (representing bores) in the solution. It is an extension into two horizontal dimensions of an earlier model used for waves on beaches (Watson et al., 1994). The boundary condition at the moving shoreline is satisfied, allowing flooding to be simulated properly. The model includes a bottom friction term but for these preliminary studies, the drag coefficient was set to zero. The model is applied to a detailed local area using a fine grid, with offshore boundary conditions provided by a surge model of a wider area including the continental shelf.

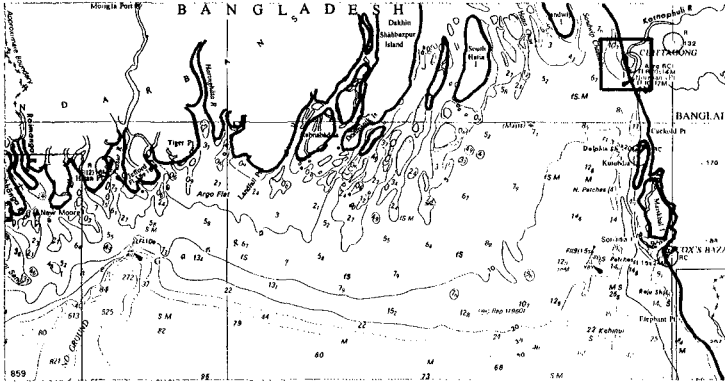Here we show results from a simulation of the flooding of Chittagong in the

Figure 2: Map of the area showing the boundaries of the large-scale storm surge model and the small-scale flooding model.
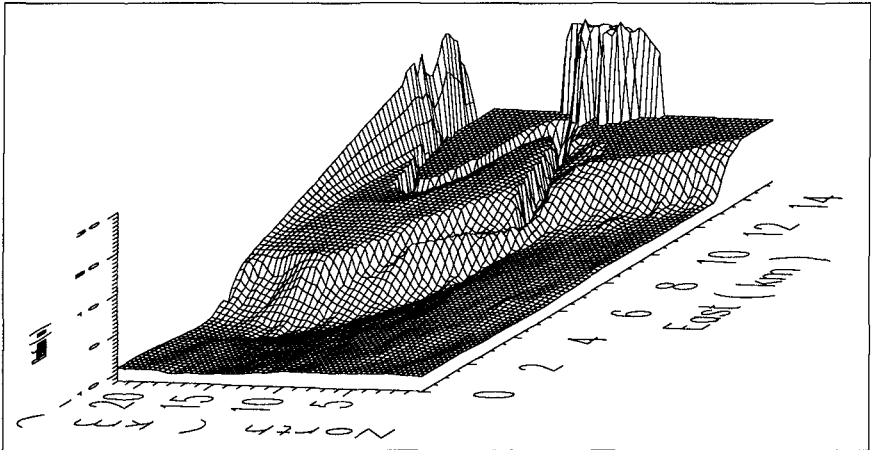

Figure 3: The topography of Chittagong and the Karnaphuli River.

April 1991 cyclone disaster in Bangladesh. A surge model of the northern Bay of Bengal (grid size 1,700 m × 1,726 m) was run using idealized pressure and wind fields based on available data for the cyclone intensity and track (Katsura et al., 1992). A fine-grid model (grid size $0.1' = 170$ m × 185 m) was then constructed for a small area around Chittagong including the Karnaphuli River, solving the nonlinear shallow-water equations. The areas covered by the two models are shown in Figure 2. A time series of water level from the surge model at the point closest to Chittagong was applied to the western boundary of the local model.

The bathymetry and topography of the local model are plotted in Figure 3.

Bathymetry data were read and interpolated manually from British Admiralty chart No. 84. It has not been possible to obtain good elevation data for the city of Chittagong, so for this preliminary study a very approximate topography was constructed. East and south of the Karnaphuli River, heights were interpolated between the water and the 25 m contour on the Admiralty chart. To the north, the 20 m contour on the Chittagong Guide Map (Govt. of Bangladesh, 1976) was used. Between coast and river, Chittagong airport was set to its elevation of 3 m. North of the airport, data were invented. This is of course an important limitation on these results, which should be taken only as an illustration of the method. An example of the results from this simulation is shown in Figure 4. Extensive flooding of Chittagong is seen, but according to Katsura et al. (1992), the flooding was not quite as extensive as is shown here.
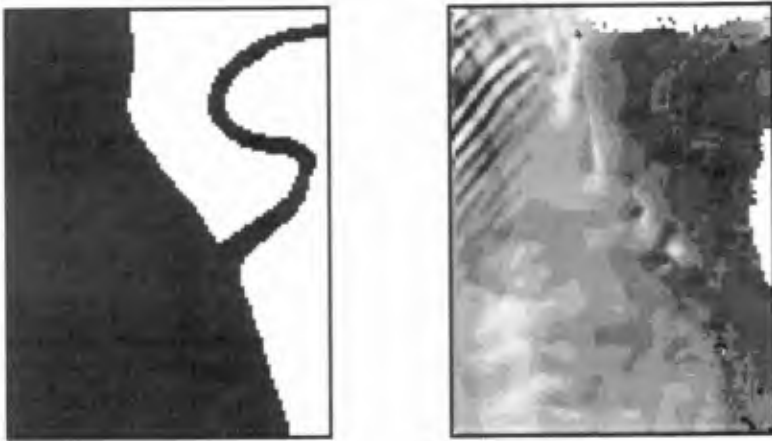

Figure 4: Preliminary results of the model showing flooding of Chittagong. *N.B. This calculation uses inaccurate topography and the result is only illustrative of the method. This result is not considered to be a good representation of the flood which actually occurred, nor of possible future floods.* On the left, the initial undisturbed state. On the right, during the storm surge flooding. Land is white and higher water levels are lighter shades.

No bore occurred in the Karnaphuli River. This is nor surprising since the river has no V-shaped estuary to concentrate the wave energy, as is common in rivers which have tidal bores. A tidal bore exists in the Meghna estuary, which was also affected by the 1991 surge, but it has so far not been possible to run the model there because of a lack of bathymetric data.

The combined model shows potential for making detailed flooding and bore formation predictions, but uncertainties remain such as how to treat buildings and different types of terrain. Unfortunately, no precise observations for testing the predictions are available. Accuracy is also limited by a lack of good topo-

graphic data for the sites of interest. Thus, it is not yet possible to apply the results with confidence to particular localities.

Wave Effects

For storm surge modelling, the most important forcing terms are the atmospheric pressure, surface wind stress and bottom friction stress. The former is of course theoretically well-defined and depends only on a reasonably accurate knowledge of the relevant time-dependent pressure field.

The stress terms represent the exchange of momentum between atmosphere and ocean, and between ocean and sea bed. Air-sea momentum exchange is a complex process involving turbulent boundary-layer flow over a changing rough surface, wave generation, non-linear energy transfer between wave components, and wave breaking. Waves also affect the bottom stress, by increasing bottom boundary later turbulence and eddy viscosity, and hence momentum transfer. These processes are not very well understood theoretically, especially in strong winds and high waves, and so are not incorporated into the models. If they can be better understood, then in principle the accuracy of the corresponding forcing terms in the models could be improved.

Dependence of Surface Wind Stress on Wave Conditions

The mean force acting on the surface of a body of water due to wind stress is usually approximated as

$$\vec{\tau}_s = \rho_a C_{D10} \vec{U}_{10} |\vec{U}_{10}| \tag{4}$$

where $\vec{\tau}_s$ is the wind stress at the surface (the horizontal force per unit area acting on the surface), ρ_a the air density, $\vec{U}_{10}$ the mean wind at 10 m and C_{D10} the drag coefficient for wind at 10 m. To represent the fact that surface roughness increases with windspeed, this coefficient is normally specified as a function of the windspeed at 10 m, $C_{D10}(U_{10})$. An example is the empirical relationship of Smith et al. (1992), which is based on data from the HEXOS experiment. This is a linear relationship given by $C_{D10} = (0.66 + 0.072U_{10}) \times 10^{-3}$. A number of similar relationships have been proposed, based on different data sets. Although the data are scattered, these empirical functions are all quite similar. This approach is a useful first approximation, and produces acceptable results in many circumstances. Note however that it applies only to well-developed seas in which the waves are approximately in equilibrium with the local wind, in deep water, and also mainly for wind speeds greater than about 5 ms^{-1}.

There may be important cases where this is inaccurate, especially if the wind is rapidly changing (such as in tropical storms), or near the coast where the water is shallow and the waves fetch-limited, or where the wave spectrum has more than one significant component. Higher values of C_D are found both in growing waves, such as during the onset of a storm, and in shallow water. Both of these conditions are necessary for the development of a storm surge, so the effect is po-

tentially important. An important parameter here is the ratio of dominant wave phase speed to wind speed, known as the wave age c_p/U, which is an indication of whether or not the wind and waves have reached equilibrium. However, what field data exist are hard to interpret because the effect is comparable in size with measurement errors, and therefore cannot be determined very accurately. It has not so far been possible to derive any empirical formulae based on the data, and so this effect is not unually incorporated into surge models. Such cases could potentially be more accurately represented by a theory which correctly accounts for momentum transfer between wind and waves, and between waves and the mean current, such as that of P. Janssen (1992). Note however that there is currently much debate on this subject, for example J. Janssen (1995) recently argued that the HEXOS data show no statistically significant dependence of wind stress on sea state.

Wind and Wave Data from the Observation Tower

This section discusses drag coefficient estimates made from observations taken by the Kyoto University DPRI Tanabe-Nakajima Storm Surge Observation Tower. The tower is located about 2 km offshore from the town of Tanabe in southern Honshu, mainland Japan. It stands at the mouth of Tanabe Bay, on a plateau about 10 m in depth, about 100 m in diameter, in an area where the depth is predominantly about 30 m. It is possible that this plateau will have some local influence on the waves, but this is difficult to determine. The tower measures wave elevation (using a downward-looking ultrasonic sea-surface height gauge), current (using an electromagnetic current meter at a depth of 10 m) and wind (using a 3-component ultrasonic anemometer at a height of 20 m). Data are recorded at 20 Hz for 20 minutes during each hour. This section discusses some drag coefficient estimates made from these data.

Because the largest surges are generated by storms, priority was given to the analysis of data from Typhoon 9426, which passed very close to the tower on 29 Sept. 1994. The lowest recorded pressure was 965 hPa at about 19:00, and the central pressure was esimated as about 950 hPa. The track was slightly south of the tower, so that the wind direction changed rapidly from east to west, also at about 19:00. Maximum recorded wind speed was 24 ms^{-1} at about 21:00. Wave height peaked at around 5 m near 17:00 and the wave period reduced from 13 s to 7 s as the typhoon passed. Direct measurements of wave direction are not available. These observations are reported in more detail by Yoshioka et al. (1995).

Following Yelland et al. (1994), wind stress was estimated from the anemometer data using the turbulent (or inertial) dissipation method. this is based on the assumption that the energy spectrum of the down-wind component is governed by the rate of dissipation of energy by high-frequency turbulence. In this case,

the spectrum is assumed to have the form:

$$S(f) = K\epsilon^{2/3} f^{-5/3} \left(\frac{U}{2\pi}\right)^{2/3} \tag{5}$$

where $S(f)$ is the power spectrum of the down-wind component, K is the 1-D Kolmogorov constant, taken as 0.55, and ϵ is the high-frequency turbulent dissipation rate. If the measured spectrum is found to obey the $f^{-5/3}$ law reasonably well, then an average value of $S(f)f^{5/3}$ over an appropriate frequency range may be used in (5) to estimate ϵ. The wind stress τ is then estimated from

$$\tau = \rho_a(k_\nu \epsilon z)^{2/3} \tag{6}$$

where k_ν is the von Kármán constant (taken as 0.4), and z is the measurement height (20 m). The drag coefficient is then obtained from (4) after correcting the observed mean wind to an estimated value at 10 m using the relation for a logarithmic boundary layer,

$$\frac{U(z)}{U(10)} = \frac{\ln(z/z_0)}{\ln(10/z_0)} \tag{7}$$

where z_0 is the roughness length $z_0 = ze^{-k_\nu/\sqrt{C_D}}$. Note that (5) applies to neutral atmospheric stability. A correction is possible for non-neutral conditions, but was found to be small in this case.
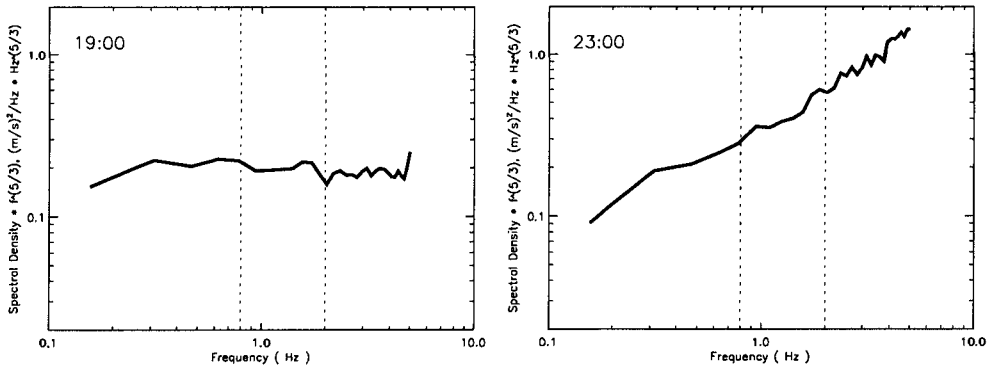

Figure 5: Wind Spectra $S(f)f^{5/3}$ at 19:00 and 23:00, 29 Sep 94 (T9426)

Figure 5 shows $S(f)f^{5/3}$ for two samples during the typhoon, at 19:00 (close the the point of closest approach) and 23:00 (a few hours after the typhoon centre passed). The plot for 19:00 is typical of those before 21:00, and the spectrum is almost constant over the frequency range used for the average (0.8–2.0 Hz, dotted

lines). This permits Eq. 5 to be used with some confidence. At 23:00 however, the spectrum exhibits a distinct slope throughout the frequency range, indicating that the $f^{-5/3}$ power law does not apply, and that (5) should not be used. Such data must be excluded from the analysis. This is unfortunate, since results just after a rapid change of wind direction are of particular interest. The reason for the different spectral slope (these data have much more high-frequency content) are not clear but may be caused by interference of the anemometer structure with the flow. One must also be aware that mean flow distortion around the tower will change the observed value of the mean wind, introducing an unknown error into the estimated drag coefficient.
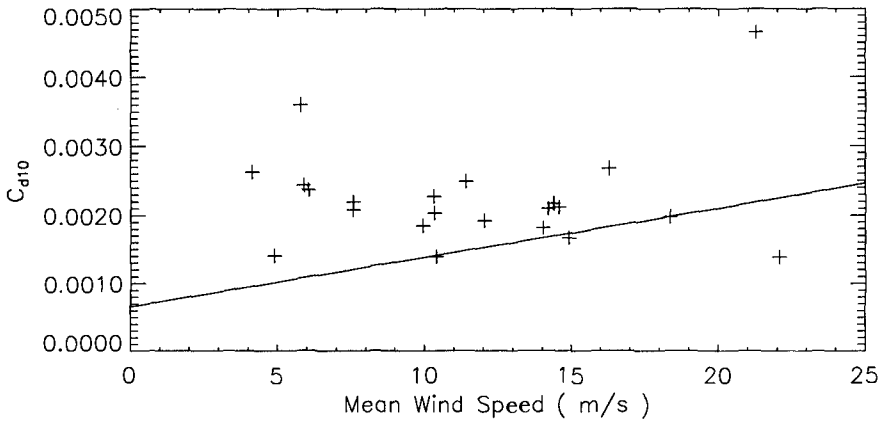

Figure 6: Drag coefficient estimates against wind speed during the typhoon.

The final estimates of stress for this day, excluding the data from 22:00 and 23:00, are plotted against mean wind speed in Figure 6 and compared with the empirical relation of Smith et al. (1992). Particularly at intermediate wind speeds, the data lie well above this curve. There is no obvious trend with wind speed, and as with other such data, they are rather scattered. If anything, a constant drag coefficient of about 2.2×10^{-3} may be appropriate in this instance. These limited data appear to be an example of departure from the standard formulae, although the whole data set should be examined before drawing firm conclusions.

Dependence of Bottom Stress on Wave Conditions

Another effect of waves which may sometimes be important is their influence on the bottom stress. In shallow water, waves affect momentum exchange with the sea bed. The wave-induced oscillatory flow near the bottom produces

turbulence when flowing over the rough bed. This increases the rate of vertical transfer of horizontal momentum, and hence the mean drag force between the water and the sea bed. Theoretically, this is represented as an increase in eddy viscosity.

In models, the mean retarding force acting on a body of water due to bottom friction is usually approximated as

$$\vec{\tau}_b = \rho_w C_{Db} \vec{u} |\vec{u}| \tag{8}$$

where $\vec{\tau}_b$ is the bottom stress, ρ the water density, $\vec{u}$ the wave-averaged bottom current and C_{Db} a bottom drag coefficient. For many applications, it is found good enough to use a constant value for C_{Db}.

The effect of wave-induced turbulence is to increase the effective value of C_{Db}. Mastenbroek (1992) estimated the size of this effect on surges in the North Sea using the relationship between drag coefficient and significant wave height, $C_{Db}(H_s)$, in Figure 3 of his paper. He found that in some shallow areas it could significantly affect the predicted surge, more so than the effect of a wave-dependent wind drag coefficient. However, the size of this effect is similar to that of geographical variations in C_{Db} due to variations in bed roughness. This makes practical implementation difficult because of the lack of sufficiently detailed data on bed roughness.

Wave Set-Up

For completeness, we also point out that another effect of waves on local water level at the coast is that of wave set-up. This may be evaluated using forcing by the gradient of radiation stresses of shoaling and breaking waves. The effect is significant in storm surges occurring on coastlines facing the open sea. Depending on the beach topography and wave conditions, this can be about 10% of the incident wave height or even more, sometimes up to about 1 m. Although not the subject of this paper, it is an effect that should also be taken into account when considering the flood risk during storms and surges.

Incorporation of Wave Effects into Surge Models

The next stage of this work, in addition to further analysis of the wind stress data, will be to incorporate wave effects into a surge model. The first step will be to use an ocean wave model suitable for the region in question, which for storm surges will usually mean shallow shelf regions with strong winds. After predicting the time-dependent wave field during the storm, the next step will be to use the results for wave height to modify the surface and bottom drag coefficients in the surge model, as outlined above. In this way, the size of wave effects on the surge prediction will be assessed.

Influence of Mountains on the Wind Field

In coastal areas with mountains, the simple formulae which are often used to

represent the wind field in tropical storms may become quite inaccurate and thus affect surge predictions. Both the shape of the mountains, and surface roughness have an effect. This is particularly so in a number of bays in Japan, such as Osaka Bay and Ise Bay, where storm surges pose a threat to low-lying urban areas. In order to reproduce the wind fields of typhoons in such places, empirical attenuation parameters have been used to decrease both the moving wind and the gradient wind, in a rough attempt to include the effects of land topography and surface roughness. However, the values have to be adjusted in each case to give results which best fit the observed wind - the best values are different for each typhoon and cannot be predicted in advance. This is unsatifsactory because it is impossible to make credible predictions for hypothetical typhoons, as for example would be desirable when planning coastal defences.

Here we improve the situation using Schloemer's equation for the typhoon pressure field, Yoshizumi's formula for the variation of wind with height in the friction layer, and a finite-difference model for air flow over topography based on mass conservation, called 'MASCON'. This model is based on Sasaki's (1970) theory and is similar to one developed by Sherman (1978), for interpolating wind vectors in complicated topography from limited wind observations.

The model works as follows. First, the equation of Schloemer (1954) is used for the atmospheric pressure as a function of distance r from the cyclone centre:

$$p = p_c + \Delta p e^{-r_m/r}. \tag{9}$$

The model of Yoshizumi (1968) is then used to evaluate the three-dimensional wind field which this would produce over a flat surface, considering the effects of surface friction (the Eckman spiral) and storm movement. This is the initial wind field for the MASCON model. The wind field is then corrected so as to satisfy the conservation of mass for an incompressible fluid, using the calculus of variations. The error of adjustment is expressed as,

$$
\begin{aligned}
E(u,v,w,\lambda) \;=\; & \int_V \Big[\alpha_1^2(u-u_0)^2 + \alpha_1^2(v-v_0)^2 + \alpha_2^2(w-w_0)^2 \\
& + \lambda \left(\frac{\partial u}{\partial x} + \frac{\partial v}{\partial y} + \frac{\partial w}{\partial z} \right) \Big] dx\,dy\,dz
\end{aligned}
\tag{10}
$$

where (u,v,w) is the corrected wind field, λ is Lagrange's indeterminate coefficient and α_1, α_2 are Gauss precision moduli. Euler-Lagrange's equations have a solution minimizing (10) which can be written as,

$$u \;=\; u_0 + \frac{1}{2\alpha_1^2} \frac{\partial \lambda}{\partial x} \tag{11}$$

$$v \;=\; v_0 + \frac{1}{2\alpha_1^2} \frac{\partial \lambda}{\partial y} \tag{12}$$

$$w \;=\; w_0 + \frac{1}{2\alpha_2^2} \frac{\partial \lambda}{\partial z} \tag{13}$$

Differentiating with respect to x, y, z respectively, and substituting into the mass conservation equation gives the following Poisson-type partial differential equation:

$$\frac{\partial^2 \lambda}{\partial x^2} + \frac{\partial^2 \lambda}{\partial y^2} + \left(\frac{\alpha_1}{\alpha_2}\right)^2 \frac{\partial^2 \lambda}{\partial z^2} = -2\alpha_1^2 \left(\frac{\partial u_0}{\partial x} + \frac{\partial v_0}{\partial y} + \frac{\partial w_0}{\partial z}\right) \tag{14}$$

This is solved for $\lambda(x, y, z)$ subject to the boundary condition

$$\frac{\partial \lambda}{\partial n} = 0 \tag{15}$$

at the boundary, where n is the coordinate normal to the boundary (for the lower boundary, this is the shape of the mountains). The solution is obtained numerically using a successive over-relaxation method.
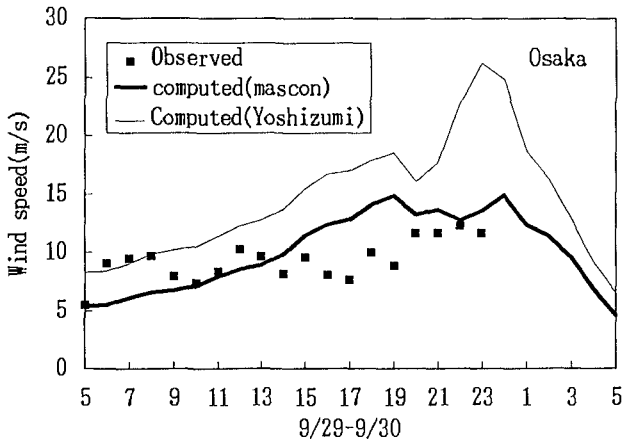

Figure 7: Observed and predicted wind speed, with and without MASCON. (Osaka, Typhoon 9426).

Wind speed and surge calculations with and without MASCON are are compared with data from Typhoon 9426 in Osaka Bay (the same typhoon as in the previous section) in Figures 7 and 8. Figure 7 shows that MASCON does not so greatly overestimate the wind speed as does Yoshizumi's model, although there is still some disagreement. Figure 8 shows that although still overpredicted, the surge result from MASCON agrees better with the measured surge. The 20 cm shift of data relative to the model results is presumed to be a temporary increase in sea level due to some event in the coastal ocean dynamics, such as a change in the Kurushio current. Similar improvements were found when this model was applied to other historical typhoons and surges in Japan.

Conclusions

The modelling of coastal flooding during storm surges may be achieved using a local model with a fine grid. This could be useful in the Bay of Bengal where the
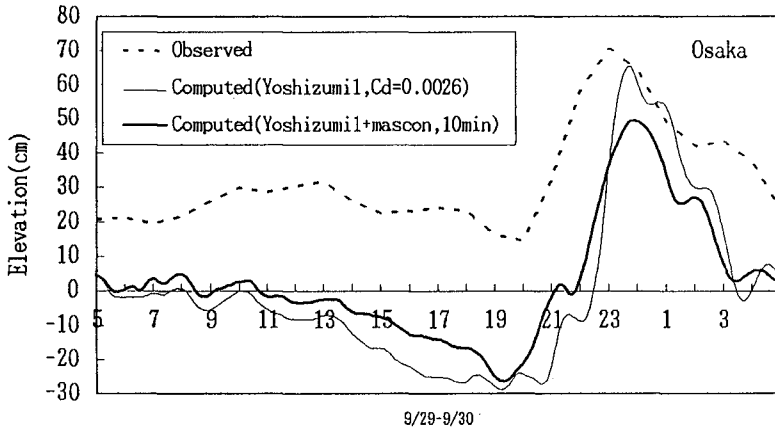
Figure 8: Observed and predicted surge, with and without MASCON. (Osaka, Typhoon 9426).

land is low, coastal defences against flooding are weak, and precise predictions of danger areas could in principle save many lives. A test case was performed for the city of Chittagong, but the results are only indicative since good land topography data were not available.

The wave field in a storm surge influences both the surface drag and, in shallow water, the bottom friction coefficients. These effects are likely to influence the size of a storm surge in some circumstances, but are not normally included in surge models. There is room for improving our understanding of the physics of these processes, especially under what circumstances they are likely to be significant. For wind stress, this should come from further collection and ananlysis of comprehensive and accurate field measurements of wind stress in a range of wind and wave conditions. Having done so, the effects may in principle be incorporated into surge models using results from an ocean wave model. Waves may also produce a measurable set-up at the coast.

Data taken during storms are particularly important for the storm surge problem. One such dataset, from a new tower, shows enhanced stress during a typhoon, in comparison with empirical formulae from the literature. Data from this tower add to those currently in existence and should be thoroughly analyzed as they become available. Eventually, a more accurate formulation of wave effects in surge models should be possible.

If there are high mountains near the coast, the resulting distortion of the wind field may have a measurable effect on the predicted surge. Using Yoshizumi's Model and the MASCON Model, a typhoon model in which the effects of both land topopgraphy and surface roughness are introduced has been developed. Hindcasts of the wind field have been made for various typhoons. These show

that even without using empirical attenuation parameters, it is possible to estimate the wind field in areas surrounded by mountains, such as Osaka Bay and Kii Channel. The predicted storm surges, although sometimes still overpredicted, also agree better with the data than the predictions of models with empirical attenuation parameters.

Acknowledgments

References

Flather, R.A. A storm surge prediction model for the northern Bay of Bengal with application to the cyclone disaster in April 1991. *J. Phys. Oceanog.* **24**, 172-190, 1994.

Janssen, J.A.M. Does wind stress depend on sea-state or not? A statistical error analysis of HEXMAX data. *KNMI preprint*, Dec. 1995.

Janssen, P.A.E.M. Quasi-linear theory of wind wave generation applied to wave forecasting. *J. Phys. Oceanogr.* **21**, 1631-1642, 1992.

Katsura, J. et al., Storm surge and severe wind disasters caused by the 1991 cyclone in Bangladesh. *Japanese Group for the Study of Natural Disaster Science, Report No. B-2*, 101 pp., 1992.

Mastenbroek, C., The effect of waves on surges in the North Sea. *Proc. 23rd Int. Conf. Coastal Eng.*, ASCE, 1992, 874-882.

Sherman, C.A., A mass-consistent model for wind fields over complex terrain. *J. Appl. Meteor.* **17**, 312-319, 1978.

Smith, S.D. et al., Sea surface wind stress and drag coefficients: the HEXOS results. *Boundary-Layer Meteorology* **60**, 109-142, 1992.

Watson, G., Barnes, T.C.D. and Peregrine, D.H., The generation of low- frequency waves by a single wave group incident on a beach. *Coastal Engineering 1994, Proc. 24th Int. Conf. Coastal Eng.*, 776-790, 1994.

Yelland, M.J. et al., The use of the inertial dissipation technique for shipboard wind stress determination. *J. Atmos. Oceanic Technology*, **11**, 1093-1108, 1994.

Yoshioka, H. et al., The storm surge induced by Typhoon 9426. (in Japanese). *Ann. Disast. Prev. Res. Inst., Kyoto Univ.*, **38**, B-2, 581-598, 1995.

Yoshizumi, S., On the asymmetry of wind distribution in the lower layer in typhoon. *J. Met. Soc. Japan*, **46**, 153-159, 1968.